



# Electroporation of the heart

Vladimir P. Nikolski, Igor R. Efimov\*

Department of Biomedical Engineering, Washington University,  
One Brookings Drive, St. Louis, MO 63130, USA

Submitted 7 January 2005, and accepted after revision 3 May 2005

## KEYWORDS

electroporation;  
defibrillation;  
optical mapping

**Abstract** Defibrillation shocks are commonly used to terminate life-threatening arrhythmias. According to the excitation theory of defibrillation, such shocks are aimed at depolarizing the membranes of most cardiac cells resulting in resynchronization of electrical activity in the heart. If shock-induced changes in transmembrane potential are large enough, they can cause transient tissue damage due to electroporation. In this review evidence is presented that (a) electroporation of the heart tissue can occur during clinically relevant intensities of the external electrical field, and (b) electroporation can affect the outcome of defibrillation therapy; being both pro- and anti-arrhythmic.

© 2005 Published by Elsevier Ltd on behalf of The European Society of Cardiology.

## Introduction

High-intensity electric shocks are commonly used in clinical practice to terminate atrial and ventricular fibrillation. Such shocks may induce pores in cellular membranes via electroporation, resulting in transient or permanent electrical and mechanical dysfunction of the heart. While high intensity shocks are used routinely, the tissue and cellular responses to large currents are not fully understood. An improved understanding of electroporation may not only reduce the side effects associated with defibrillation therapy but also may help in designing more effective ways to deliver genes and drugs to target cells. In this

paper, we review the available literature on electroporation in the heart and relate the findings to several recent experimental studies performed in our laboratory.

## Cellular responses to strong electric fields

Electroporation has been most extensively studied in bilayer systems [1,2]. These systems allow for precise control of transmembrane voltage along with adequate dynamic range and temporal resolution of recordings of the characteristics of electric conduction through the pore, induced by electric stimuli. Such experimental studies provide a detailed description of the process of electroporation and resealing of the pores. Electroporation has also been characterized quantitatively in

\* Corresponding author. Tel.: +1 216 368 1916; fax: +1 216 368 5143.

E-mail address: ire@cwru.edu (I.R. Efimov).

isolated cardiac cells [3,4]. Experimental observations have allowed construction of mathematical models of the behaviour of a single pore [5–7] and the participation of pores in the electrical activity of cardiac myocytes [4,8,9] and of the tissue [10,11] during strong electric field stimulation.

Rapid-freezing electron microscopy of cells rendered electroporeable provided direct evidence of the formation of Volcano-shaped pores in cell membranes [12]. However, direct real-time recording or visualization of electroporation in vivo or in vitro tissue or organ systems remains to be developed. Presently, information about electroporation can be indirectly inferred from [13] tissue staining with fluorescent dyes which can penetrate the cells only through the pores, and subsequent histological intracellular imaging; and from electroporation-induced depression of excitability [2] resulting in depolarization of the cellular membrane during the diastolic interval [3,13–15], reduction of amplitude of action potentials and of the rate of rise of their upstroke ( $dV/dt$ ) (Fig. 1), and elevation of intracellular calcium concentration [3].

In whole cell patch-clamp experiments, during application of increasing voltages, the cellular membrane experiences an abrupt, step decrease in resistance [16], which is unaffected by Na, K, and Ca channel blockers [17]. This result is consistent with the formation of ion-nonspecific membrane pores. Application of this technique for detection of electroporation in the tissue is difficult because the reduction in cell membrane resistance is translated only into a small decrease in the total tissue resistance. Additionally, previous modelling work has shown that electroporation occurs only in a very small amount of tissue, perhaps only a one-cell layer adjacent to the electrode [10,11].

### Electroporation assessment via shock induced transmembrane

Double-barrelled microelectrode recordings and optical mapping techniques showed that weak stimuli, as predicted by the cable theory and generalized activating function theory, produce

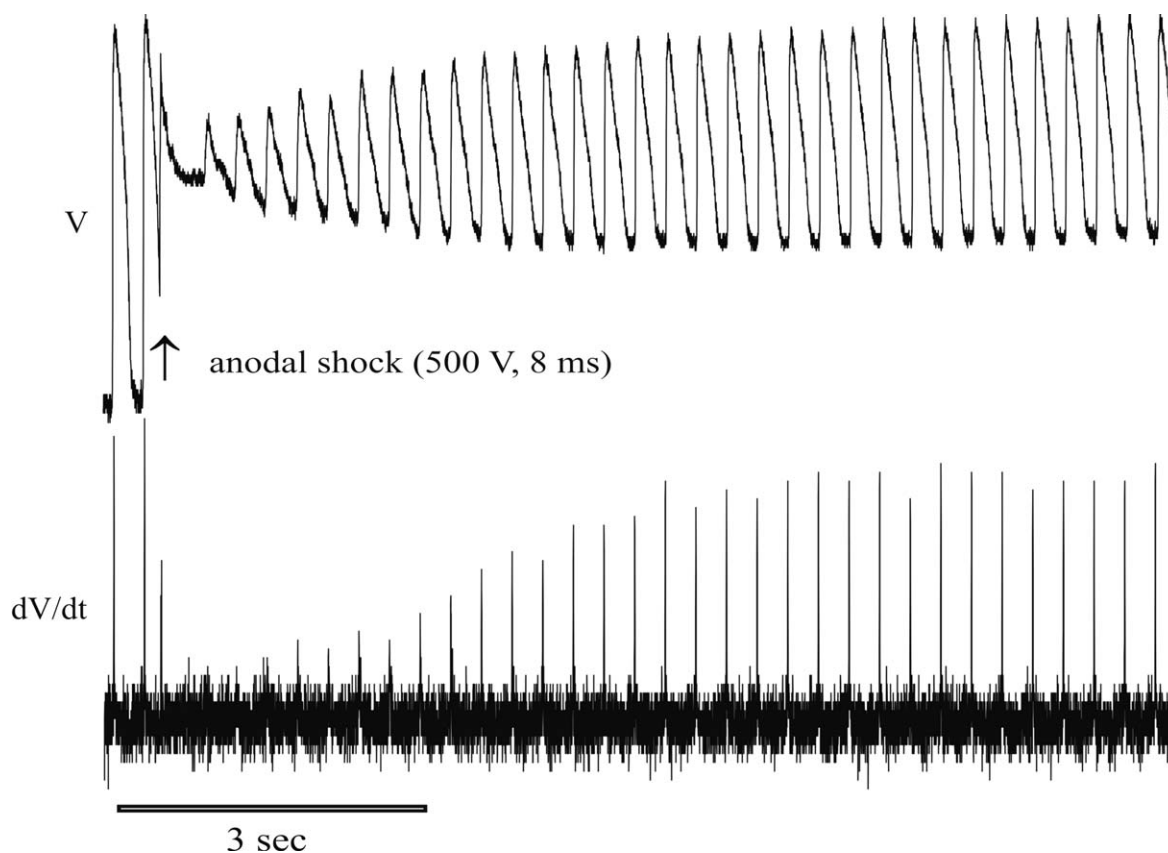


**Figure 1** Evidence of shock-induced electroporation. Optical recording of transmembrane potential,  $V$  (upper trace), shows time-dependent post-shock reduction of resting potential and action potential amplitude. Maximal upstroke rate of rise ( $dV/dt$ ) is also reduced and slowly recovers after shock (lower trace). Reproduced with permission [13].

monotonic transmembrane potential changes ( $\Delta V_m$ ) in a single cell [18,19], cell culture strands [20], and heart tissue [21,22]. However, reports on strong shocks of defibrillation strength sharply disagree on the morphology and amplitude of shock-induced response  $\Delta V_m$ . When a stimulus is applied to a single cell during the early plateau phase of the action potential, the optical recordings show depolarization of the cathodal end and hyperpolarization of the anodal end of the cell [23,24].

When the stimulus intensity increases, the induced hyperpolarization (or more accurately negative polarization)  $\Delta V_m$  first gradually increases in amplitude but soon starts to decay, causing elevation of cell average potential, Fig. 2 [19]. Similar effects were observed in narrow strands of cultured rat myocytes [20]. It was suggested that electroporation was a likely mechanism of non-monotonic hyperpolarization transients.

More direct evidence was needed. One such verification might be dye uptake through pores induced by electroporation. Uptake depends on dye concentration differences inside and outside the cells and of the net electrical charge of the dye. Because Lucifer Yellow dye uptake was not

observed at 50 V/cm shock strength, which was above the 30V/cm threshold of non-monotonic negative  $\Delta V_m$ , the conclusion was not definitive and an activation of an unknown hyperpolarization-activated channel(s) was proposed as an alternative explanation [25]. More recently this same group has detected such uptake using another indicator: propidium iodide [26]. However, Gillis et al. [27] did observe an accumulation of Lucifer Yellow dye in areas close to the anode and cathode after shocks with a field strength  $\geq 22$  V/cm in a similar experimental design. Currently, the appearance of the second phase of hyperpolarizing transients (see labels 1,2 in Fig. 2A) is considered a signature of membrane electroporation.

The lack of detectable dye uptake in some of the previous studies could be related to the small exposure time and to the lower sensitivity of the Lucifer Yellow technique. Propidium iodide has 20–30 fold increases in fluorescence after binding to nucleic acids. In contrast to negative response  $\Delta V_m$ , positive polarization in a single cell and in cell culture was found to increase gradually with shock strength, saturating below 100% of action potential amplitude (APA) [20].

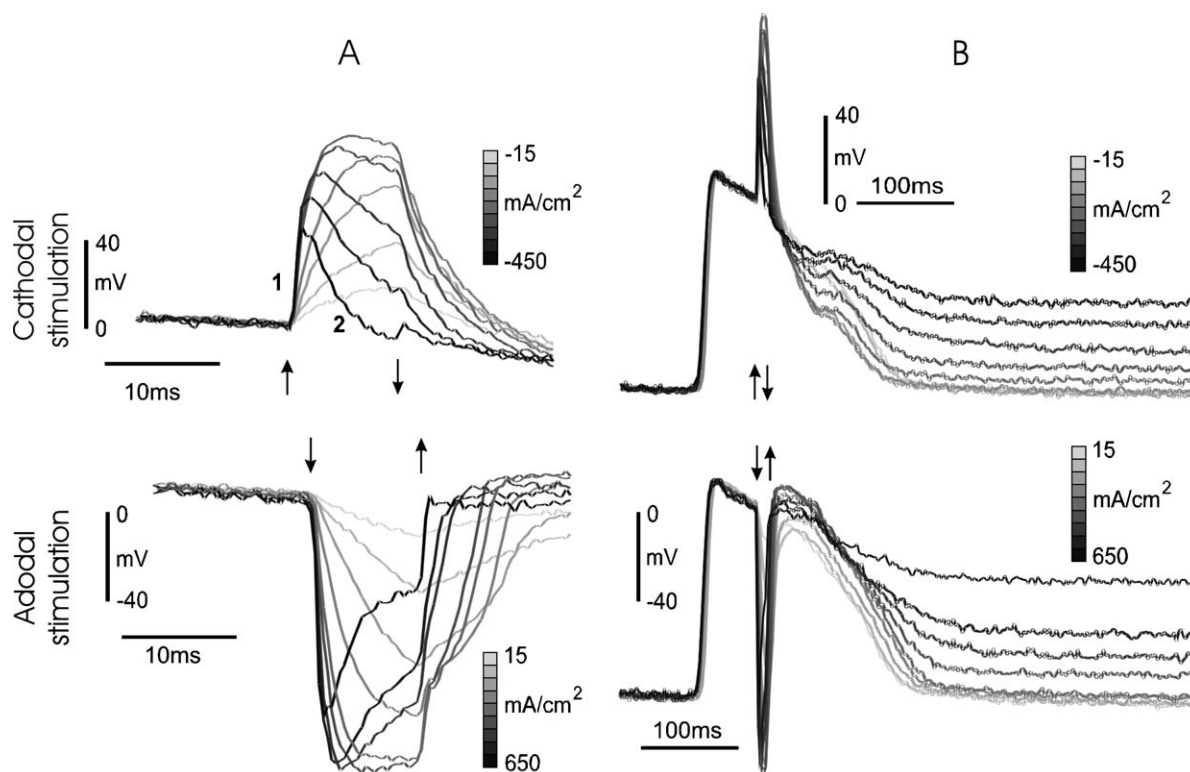


**Figure 2** Optical recording of transmembrane potential transients under the electrode during stimulation with different current densities. A, small time scale; B, large time scale. Arrows mark stimulus onset and withdrawal. Current strength is grey-scale coded. Electroporation is evident from saturation of  $\Delta V_m$  and elevation of the diastolic potential. Reproduced with permission [38].

Whole heart studies revealed different types of asymmetry for the positive and negative polarizations during strong shocks (see Fig. 2). In a recent study [28], we also found that these effects are accompanied by epicardial post-shock elevation of diastolic potential (DP) (see Fig. 2, right panels). In our study, we determined epicardial  $\Delta V_m$  responses during high-density electric current stimuli of both polarities applied at the 6 mm diameter area of the left ventricle. We detected saturation and subsequent decay of epicardial polarizations during strong cathodal and anodal shocks applied at the area with a size of several space constants (0.8–1.5 mm at the epicardium [29]). Our optical recordings of negative  $\Delta V_m$  responses to high-intensity stimuli were in agreement with the results reported by others in strands of cultured myocytes [20,30], single cell [4], and frog heart [15] for hyperpolarizing stimuli. We did not observe a plateau or an increase in the depolarization transients during cathodal stimuli for the same stimulus strengths that caused a decayed hyperpolarization response. Neunlist and Tung [15] presented measurements of epicardial cellular responses recorded from 150  $\mu\text{m}$  diameter area of stimulus application, showing hyperpolarization overshoot during anodal stimulation [16], similar to that found in cell strands [20,25].

Recent data [22] from Fast et al. showed that the initial positive polarization in virtual cathode areas in a wedge preparation changes to hyperpolarizing responses as the stimulus strength increases to 30 V/cm and above, similar to the behaviour of the middle of a single myocyte in studies by Sharma and Tung [19]. Such observations were reported previously by Cheng et al. [31] and Zhou et al. [32], who detected hyperpolarization transients near the cathodal shock electrode. We observed the same phenomena in optical recordings from the epicardial surface [28]. This can explain why depolarization saturation is observed at lower shock current densities than hyperpolarization saturation. Neunlist and Tung [15] stimulated a small area near the electrode that could affect their measurements due to a virtual electrode effect [33], leading to development of positive and negative polarizations at nearby locations. In contrast, our experiments were designed to overcome this limitation by stimulating a large area relative to the field of view. Similarly, we did not use transmural sections of tissue, which will interrupt fibres and thus could affect the results in a slab preparation [33]. However, a strong cathodal stimulus resulted in hyperpolarizing responses and this response was partially reversible. We considered electropora-

tion as the most plausible explanation of these effects. However, it would require voltage-dependent resealing of the pores during the shock application to explain the restoration of the membrane resistance.

The correlation between anodal (negative)  $\Delta V_m$  and diastolic  $V_m$  elevation was recently reported by Fast and Cheek [25] in myocyte cultures. A similar result was shown earlier by Neunlist and Tung [15] and Cheng et al. [31]. Interestingly, Fast and Cheek [25] did not observe non-monotonic  $\Delta V_m$  at the cathodal end of the cell strand even at the highest shock strengths. A possible explanation for the absence of positive  $\Delta V_m$  decay in the Fast and Cheek [25] study was recently suggested by these authors [34,35]. They demonstrated that the absence of positive polarizations in optical recording of transmembrane potential at the edge of the preparation facing the cathodal electrode during strong shocks results from the spatial averaging of polarization in the neighbouring areas.

In our study, both stimuli polarities had the same injury threshold, judging by diastolic potential elevation [28]. Our findings agree with earlier reports by Knisley and Grant, who showed that cell injury is independent of the intrinsic transmembrane potential [36]; and by Moroz et al., who reported the same electroporation threshold for monophasic and biphasic shock waveforms [37]. These reports contradict results obtained in the single cell and in cell cultures, in which anodal sides of single cells or cell strands were affected more significantly than cathodal sides [25,36].

Application of a Ca-channel blocker resulted in an increase in the saturation level of depolarizing responses and did not affect hyperpolarizing responses in cell culture [30]. Despite the differences in the depolarization transients behaviour mentioned above, we observed that nifedipine increased the saturation levels for positive but not negative  $\Delta V_m$  also during epicardial stimulation. Ca-channel blockers did not affect the electroporation threshold in whole cell patch studies [17] and only increased positive  $\Delta V_m$  in cell culture studies [30]. Yet, there is a clear effect of nifedipine on the saturation level for the depolarization signal in our study, which means that other factors (i.e. space averaging in optical recordings) could also be responsible for saturation and reversal of the depolarizing responses with stimulus strength increase.

In agreement with earlier reports [15,16], we observed that a rather small optical hyperpolarization response could be sufficient for electroporation. Among possible reasons for this were (a) a 'dog-bone' virtual polarization near the

spacing electrode [15] that could attenuate the response due to optical averaging over areas of opposite polarizations, or (b) insufficient temporal resolution of our optical mapping system [15] that could underestimate the true instantaneous transmembrane voltage produced by a square pulse. Our results for polarization transients recorded during 10 ms ramp waveform stimulation (no temporal resolution limitations) over a 6 mm diameter area of epicardium (opposite polarization is located 3 mm away from the central recording point) reject such explanations.

### Electroporation assessment by membrane impermeable dye diffusion

The most convincing indicator of electroporation is shock-induced facilitation of transport of macromolecules across the cell membrane. Despite the fact that this method of making the cell permeable is already a routine technique, the complete understanding of its mechanisms remains to be formulated. The most fundamental questions remain unknown: what is the size and density of pores created by the shock, do pores grow after the shock, and what is the time course of their resealing? In our experiments with propidium iodide (PI) we did not detect an immediate PI fluorescence increase during the shock. This suggests that the amount of PI molecules that penetrated

through the electroporation holes during the 20 ms stimulus was undetectable in our protocol. This also explains why we did not observe a difference in PI uptake for shocks of different polarities despite the positive charge of the PI molecule. Slow diffusion of PI into the cells takes place when the external electrical field is turned off, thus fluorescence is continuously rising after the shock during dye perfusion in our experiments [38] as it did in cell culture studies [39]. These data suggest that in our experiments, electroporated cells were repaired within minutes rather than seconds. In our study, we observed the PI dye uptake at a shock strength of 700 mA/cm<sup>2</sup> (35V/cm) when we detected non-monotonic  $\Delta V_m$ , and no PI uptake at 300 mA/cm<sup>2</sup> (15 V/cm) when  $\Delta V_m$  was monotonic (see Fig. 3). We suggest that DP elevation might be a more sensitive indicator of electroporation than PI uptake because DP elevation can be detected within one second after shock application. However, this method cannot be used at depth in three-dimensional tissues.

While PI is used widely in electroporation research, these studies are usually conducted on cell suspensions. There were concerns that this molecule may not be well suited to studies in tissues with interconnected cells due to its relatively small molecular weight (668 Da) with a radius about 0.6 nm, which is smaller than the pore of a gap junction channel (about 0.8 nm). Thus, it was suggested that PI might diffuse into neighbouring

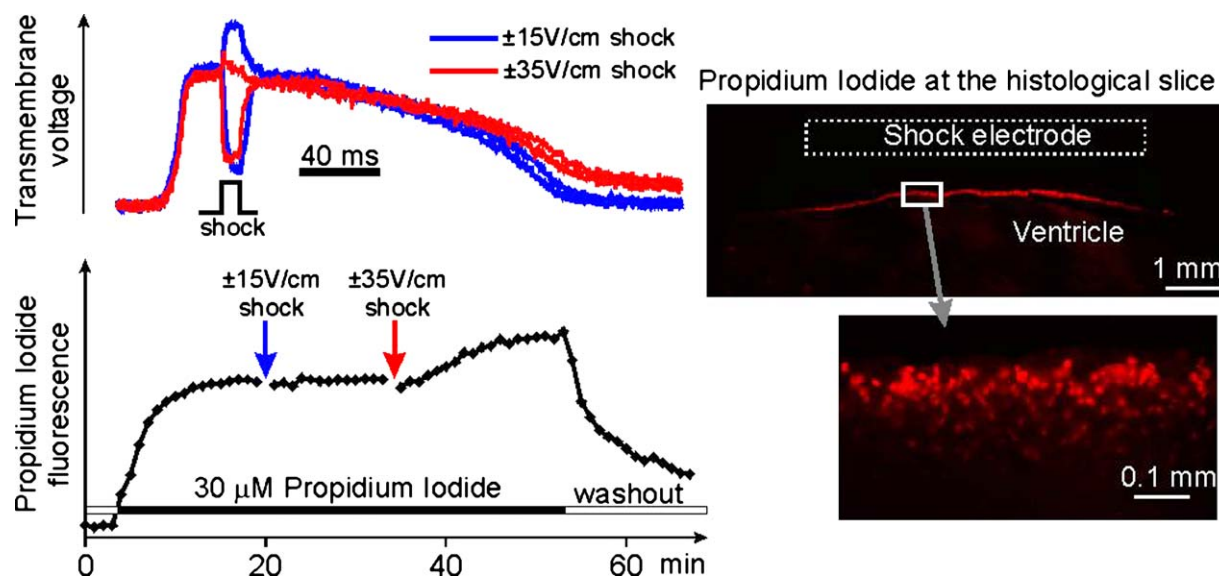


**Figure 3** Manifestation of electroporation changes in optical potential recordings is associated with an increase of propidium iodide fluorescence under the stimulation electrode. No increase was observed at sites not under the electrode. Histological images showed typical pattern of nuclear stain in the thin layer of epicardium at the areas where optical potentials had signs of electroporation. Reproduced with permission [38].

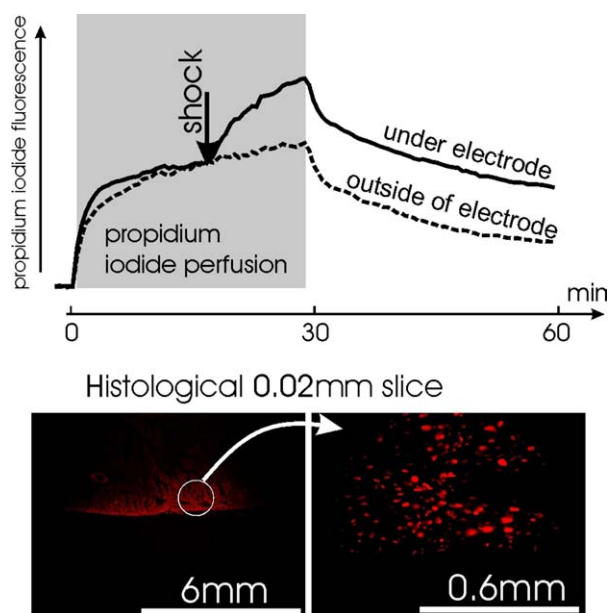


**Figure 4** Uptake of membrane impermeable dye propidium iodide after a strong shock. Upper panel shows the initial increase in propidium iodide fluorescence, after the beginning of perfusion, recorded inside the stimulated area and 3 mm outside the stimulated area. After shock application ( $1600 \text{ mA/cm}^2$ , 20 ms), there was an accelerated accumulation of fluorescence in the stimulated tissue. Lower panel shows the fluorescent images made with  $4\times$  and  $40\times$  lenses for  $20 \mu\text{m}$  slices sectioned throughout the stimulated area. The electroporated region is clearly demarcated by the propidium iodide-stained cell nuclei. Reproduced with permission [38].

cells, creating an appearance of electroporation in intact cells.

Our data show significant differences in the depth of staining with PI, including staining of some interior regions of myocardium, which are isolated from other stained regions. The area of electroporation, identified by PI staining, which occurred in the middle of the papillary muscle confirms that in our experiments diffusion extends less than  $0.1 \text{ mm}$ . Diffusion of PI molecules is theoretically possible through gap junctions. But perhaps it does not occur over large distances due to rapid binding of PI to the nuclei, which prevents its diffusion in the intracellular space (Fig. 4).

A single cell study showed that during  $2 \text{ kV/cm}$ ,  $20 \mu\text{s}$  shocks, the cells with irreversible membrane electroporation accumulate a 5-times larger amount of PI than cells that restored their membrane within 10 min after field exposure [39]. It was also shown that  $1.8 \text{ A/cm}^2$  stimuli cause irreversible cell damage [40]. This indicates that PI accumulation during the strong shock

could be related to other factors (barotrauma, hyperthermia) leading to cell death. If such factors are less dependent on proximity to the tissue boundaries than electroporation [10,11], they can explain the much larger depth of affected tissue after  $1.6 \text{ A/cm}^2$  shock in comparison with the  $0.7 \text{ A/cm}^2$  shock.

## Tissue responses to strong electric field

The main interest in studying the effects of electrical shocks on the heart was driven by the ability of strong shocks to terminate arrhythmias. Two major, competing theories — the incapacitation theory [41] and the stimulation theory [42] — have been used to explain defibrillation success.

We believe that the two theories of defibrillation are extreme in their assessment of the role of electroporation. Incapacitation theory places electroporation as the foundation of the mechanisms of defibrillation, while stimulation theory ignores the role of electroporation in defibrillation. The truth is likely to be between these two extremes. Despite significant improvement in defibrillation efficacy, which resulted in a radical reduction of defibrillation thresholds and myocardial damage, there is still extensive clinical and basic electrophysiology data indicating that defibrillation shocks are accompanied by adverse effects. These effects are likely to be associated with electroporation and may include: (1) transient ectopy, tachycardia or induction of ventricular fibrillation [25,43,44]; (2) depression of electrical and mechanical functions [13–15,45,46]; (3) bradycardia, complete heart block and increased pacing thresholds [44,47,48]; (4) atrial and ventricular mechanical dysfunction (stunning), which is directly related to the strength of shocks [49–52]; (5) significant elevation of Troponin I serum level in patients after spontaneous cardioverter defibrillator shocks [53]; (6) decrease in the myocardial lactate extraction rate by mitochondria [54].

Both clinical and basic experimental evidence suggests that electroporation is induced [55] by defibrillation shocks, and plays a role in defibrillation [56] and post-shock metabolism and electromechanical function of the heart. However, the anti-fibrillatory role of electroporation is not clear, since conflicting data suggest both pro- and anti-arrhythmic effects of electroporation [13,14].

Understanding the effects of electroporation in cardiac tissue or the whole heart levels during application of an external electric field is much

less developed than for single cell experiments. One of the problems of such experiments is related to the strong spatial heterogeneity of electroporation effects, which complicate their interpretation [13–16].

Several of our own studies were aimed at exploring spatio-temporal patterns and voltage dependence of electroporation in several types of preparations, such as the whole, intact Langendorff-perfused heart [13,31], the isolated endocardium and septum preparations [13], and 6 mm diameter areas of epicardium under the stimulating electrode [57]. In these studies, we found that electroporation is dependent upon shock intensity, tissue structure and electrode configuration. For example, we found that the endocardium is significantly more susceptible to electroporation than the epicardium [13].

Electroporation can selectively affect small trabeculated structures and bundles of the conduction system of the heart. This could result in transient suppression of excitability and conduction block [46]. We found that conduction in a small papillary muscle in the rabbit heart can be transiently inhibited by a strong electric shock. We found that such transient block can last from one beat to many seconds, depending on the shock strength [13]. Potentially, such transient inhibition of conduction in conduction bundles of the heart can lead to initiation of a re-entrant or focal arrhythmia, or on the other hand, can have an anti-arrhythmic effect by isolation of ectopic foci and the reduction of tissue mass available for arrhythmia maintenance.

Profibrillatory effects of electroporation and tissue damage are supported by clinical observations of post-shock ectopy and arrhythmia as reviewed above, as well as by basic studies including the classical studies of Gurvich [58], as well as several recent studies [14,25,59]. Anti-fibrillatory effects of electroporation have been known since the seminal work of Prevost and Battelli [41]. We also obtained data that support anti-fibrillatory effects of electroporation [13]. Our results [13] show that a strong electroporating shock reduces vulnerability to shock-induced arrhythmia applied during a period of electroporation.

A test shock applied during the T wave induces arrhythmias in 94.8% of cases without a preconditioning shock (Fig. 5, left bar). Most of these arrhythmias are sustained (grey bar). Application of the preconditioning shock with an intensity equal to DFT reduces inducibility to 70%. Application of the electroporating preconditioning shock with an intensity equal to 3×DFT completely eliminates vulnerability.

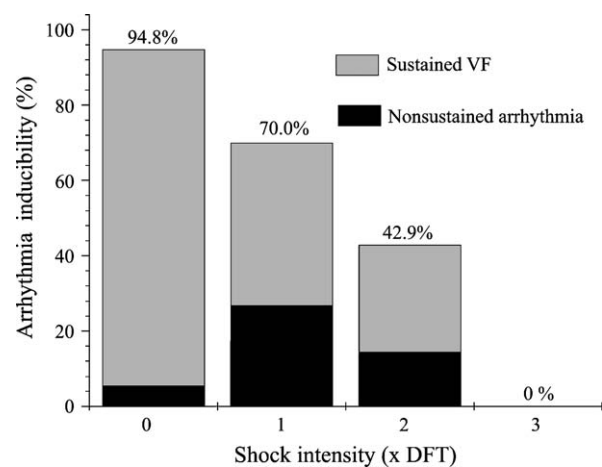


**Figure 5** Inducibility of ventricular fibrillation by T-wave shock versus preconditioning shock applied 1200 or 1500 ms before. Preconditioning shock intensity is expressed as 0×, 1×, 2×, 3× defibrillation thresholds. Reproduced with permission [13].

## Conclusion

Application of electrical shocks is a routine technique to treat cardiac arrhythmias. High-intensity fields generated inside cardiac tissue cause transient tissue damage due to electroporation. Electroporation can be monitored by changes in the morphology of the transmembrane polarization transients during anodal and cathodal shocks from monotonic to non-monotonic responses, elevation of the resting potential, and post-shock AP amplitude reduction. Electroporation changes in transmembrane potential traces are present for hyperpolarized as well as depolarized stimuli of a similar strength. Membrane impermeable dye (i.e. propidium iodide) uptake signifies that recovery of membrane integrity in cardiac cells can take minutes after shock termination. Such long-lasting effects can have both anti- and pro-arrhythmic effects in the heart. Further improvement in defibrillation therapy may be able to direct electroporation power precisely to the re-entry substrate in order to minimize the adverse effects on cardiac contractile properties or for delivering gene therapy to the arrhythmogenic zones.

## Acknowledgements

This work was supported by National Heart, Lung, and Blood Institute Grants R01HL-67322 and R01HL-074283.

## References

- [1] Tung L, Troiano GC, Sharma V, Raphael RM, Stebe KJ. Changes in electroporation thresholds of lipid membranes by surfactants and peptides. *Ann N Y Acad Sci* 1999;888:249–65.
- [2] Melikov KC, Frolov VA, Shcherbakov A, Samsonov AV, Chizmadzhev YA, Chernomordik LV. Voltage-induced non-conductive pre-pores and metastable single pores in unmodified planar lipid bilayer. *Biophys J* 2001;80:1829–36.
- [3] Krauthamer V, Jones JL. Calcium dynamics in cultured heart cells exposed to defibrillator-type electric shocks. *Life Sci* 1997;60:1977–85.
- [4] Cheng DK, Tung L, Sobie EA. Nonuniform responses of transmembrane potential during electric field stimulation of single cardiac cells. *Am J Physiol* 1999;277:H351–62.
- [5] Krassowska W, Neu JC. Response of a single cell to an external electric field. *Biophys J* 1994;66:1768–76.
- [6] Chizmadzhev YA, Kuzmin PI, Kumenko DA, Zimmerberg J, Cohen FS. Dynamics of fusion pores connecting membranes of different tensions. *Biophys J* 2000;78:2241–56.
- [7] Smith KC, Neu JC, Krassowska W. Model of creation and evolution of stable electropores for DNA delivery. *Biophys J* 2004;86:2813–26.
- [8] DeBruin KA, Krassowska W. Modelling electroporation in a single cell. II. Effects of ionic concentrations. *Biophys J* 1999;77:1225–33.
- [9] DeBruin KA, Krassowska W. Modelling electroporation in a single cell. I. Effects of field strength and rest potential. *Biophys J* 1999;77:1213–24.
- [10] Aguel F, DeBruin KA, Krassowska W, Trayanova NA. Effects of electroporation on the transmembrane potential distribution in a two-dimensional bidomain model of cardiac tissue. *J Cardiovasc Electrophysiol* 1999;10:701–14.
- [11] DeBruin KA, Krassowska W. Electroporation and shock-induced transmembrane potential in a cardiac fiber during defibrillation strength shocks. *Ann Biomed Eng* 1998;26:584–96.
- [12] Chang DC, Reese TS. Changes in membrane structure induced by electroporation as revealed by rapid-freezing electron microscopy. *Biophys J* 1990;58:1–12.
- [13] Al-Khadra AS, Nikolski V, Efimov IR. The role of electroporation in defibrillation. *Circ Res* 2000;87:797–804.
- [14] Kodama I, Shibata N, Sakuma I, Mitsui K, Iida M, Suzuki R, et al. Aftereffects of high-intensity DC stimulation on the electromechanical performance of ventricular muscle. *Am J Physiol* 1994;267:H248–58.
- [15] Neunlist M, Tung L. Dose-dependent reduction of cardiac transmembrane potential by high-intensity electrical shocks. *Am J Physiol* 1997;273:H2817–25.
- [16] Tung L, Tovar O, Neunlist M, Jain SK, O'Neill RJ. Effects of strong electrical shock on cardiac muscle tissue. *Ann N Y Acad Sci* 1994;720:160–75.
- [17] Tovar O, Tung L. Electroporation and recovery of cardiac cell membrane with rectangular voltage pulses. *Am J Physiol* 1992;263:H1128–36.
- [18] Gray RA, Huelsing DJ, Aguel F, Trayanova NA. Effect of strength and timing of transmembrane current pulses on isolated ventricular myocytes. *J Cardiovasc Electrophysiol* 2001;12:1129–37.
- [19] Sharma V, Tung L. Spatial heterogeneity of transmembrane potential responses of single guinea-pig cardiac cells during electric field stimulation. *J Physiol* 2002;542:477–92.
- [20] Fast VG, Rohr S, Ideker RE. Nonlinear changes of transmembrane potential caused by defibrillation shocks in strands of cultured myocytes. *Am J Physiol Heart Circ Physiol* 2000;278:H688–97.
- [21] Efimov IR, Cheng YN, Biermann M, Van Wagoner DR, Mazgalev T, Tchou PJ. Transmembrane voltage changes produced by real and virtual electrodes during monophasic defibrillation shock delivered by an implantable electrode. *J Cardiovasc Electrophysiol* 1997;8:1031–45.
- [22] Fast VG, Sharifov OF, Cheek ER, Newton JC, Ideker RE. Intramural virtual electrodes during defibrillation shocks in left ventricular wall assessed by optical mapping of membrane potential. *Circulation* 2002;106:1007–14.
- [23] Knisley SB, Blitchington TF, Hill BC, Grant AO, Smith WM, Pilkington TC, et al. Optical measurements of transmembrane potential changes during electric field stimulation of ventricular cells. *Circ Res* 1993;72:255–70.
- [24] Windisch H, Ahammer H, Schaffer P, Muller W, Platzer D. Optical multisite monitoring of cell excitation phenomena in isolated cardiomyocytes. *Pflügers Arch* 1995;430:508–18.
- [25] Fast VG, Cheek ER. Optical mapping of arrhythmias induced by strong electrical shocks in myocyte cultures. *Circ Res* 2002;90:664–70.
- [26] Cheek ER, Fast VG. Nonlinear changes of transmembrane potential during electrical shocks: role of membrane electroporation. *Circ Res* 2004;94:208–14.
- [27] Gillis AM, Fast VG, Rohr S, Kleber AG. Spatial changes in transmembrane potential during extracellular electrical shocks in cultured monolayers of neonatal rat ventricular myocytes. *Circ Res* 1996;79:676–90.
- [28] Nikolski VP, Sambelashvili AT, Krinsky VI, Efimov IR. Effects of electroporation on optically recorded transmembrane potential responses to high-intensity electrical shocks. *Am J Physiol Heart Circ Physiol* 2004;286:H412–8.
- [29] Akar FG, Roth BJ, Rosenbaum DS. Optical measurement of cell-to-cell coupling in intact heart using subthreshold electrical stimulation. *Am J Physiol Heart Circ Physiol* 2001;281:H533–42.
- [30] Cheek ER, Ideker RE, Fast VG. Nonlinear changes of transmembrane potential during defibrillation shocks: role of  $Ca^{2+}$  current. *Circ Res* 2000;87:453–9.
- [31] Cheng Y, Tchou PJ, Efimov IR. Spatio-temporal characterization of electroporation during defibrillation. *Biophys J* 1999;76:A85 [abstract].
- [32] Zhou X, Ideker RE, Blitchington TF, Smith WM, Knisley SB. Optical transmembrane potential measurements during defibrillation-strength shocks in perfused rabbit hearts. *Circ Res* 1995;77:593–602.
- [33] Neunlist M, Tung L. Spatial distribution of cardiac transmembrane potentials around an extracellular electrode: dependence on fiber orientation. *Biophys J* 1995;68:2310–22.
- [34] Fast VG, Cheek ER, Pollard AE, Ideker RE. Effects of electrical shocks on  $Ca^{2+}$  and  $V_m$  in myocyte cultures. *Circ Res* 2004;94:1589–97.
- [35] Sharifov OF, Ideker RE, Fast VG. High-resolution optical mapping of intramural virtual electrodes in porcine left ventricular wall. *Cardiovasc Res* 2004;64:448–56.
- [36] Knisley SB, Grant AO. Asymmetrical electrically induced injury of rabbit ventricular myocytes. *J Mol Cell Cardiol* 1995;27:1111–22.
- [37] Moroz VV, Bogushevich MS, Chernysh AM, Kozlova EK, Sharakshane AS. Effect of defibrillation pulses of different shapes on biomembranes: experimental study. *Bull Exp Biol Med* 2004;137:120–3.
- [38] Nikolski VP, Sambelashvili AT, Krinsky VI, Efimov IR. Effects of electroporation on optically recorded transmembrane potential responses to high-intensity electrical shocks. *Am J Physiol Heart Circ Physiol* 2004;286:H412–8.

- [39] Shirakashi R, Kostner CM, Muller KJ, Kurschner M, Zimmermann U, Sukhorukov VL. Intracellular delivery of trehalose into Mammalian cells by electropermeabilization. *J Membr Biol* 2002;189:45–54.
- [40] Koning G, Veefkind AH, Schneider H. Cardiac damage caused by direct application of defibrillator shocks to isolated Langendorff-perfused rabbit heart. *Am Heart J* 1980;100:473–82.
- [41] Prevost JL, Battelli F. Sur quelques effets des decharges electriques sur le coeur mammifres. *Comptes Rendus Seances Acad Sci* 1899;129:1267.
- [42] Gurvich NL, Yuniev GS. Restoration of regular rhythm in the mammalian fibrillating heart. *Byulletin Eksper Biol Med* 1939;8:55–8.
- [43] Donoso E, Cohn LJFK. Ventricular arrhythmias after precordial electric shock. *Am Heart J* 1967;73:595–601.
- [44] Waldecker B, Brugada P, Zehender M, Stevenson W, Welens HJ. Ventricular arrhythmias after precordial electric shock. *Am J Cardiol* 1986;57:120–3.
- [45] Tovar O, Tung L. Electroporation of cardiac cell membranes with monophasic or biphasic rectangular pulses. *Pacing Clin Electrophysiol* 1991;14:1887–92.
- [46] Yabe S, Smith WM, Daubert JP, Wolf PD, Rollins DL, Ideker RE. Conduction disturbances caused by high current density electric fields. *Circ Res* 1990;66:1190–203.
- [47] Eysmann SB, Marchlinski FE, Buxton AE, Josephson ME. Electrocardiographic changes after cardioversion of ventricular arrhythmias. *Circulation* 1986;73:73–81.
- [48] Stickney RE, Doherty A, Kudenchuk PJ, Morud SA, Walker C, Chapman FW, et al. Survival and postshock ECG rhythms for out-of-hospital defibrillation. *Pacing Clin Electrophysiol* 1999;22:740 [abstract].
- [49] Sparks PB, Kulkarni R, Vohra JK, Mond HG, Jayaprakash S, Yapanis AG, et al. Effect of direct current shocks on left atrial mechanical function in patients with structural heart disease. *J Am Coll Cardiol* 1998;31:1395–9.
- [50] Sparks PB, Jayaprakash S, Mond HG, Vohra JK, Grigg LE, Kalman JM. Left atrial mechanical function after brief duration atrial fibrillation. *J Am Coll Cardiol* 1999;33:342–9.
- [51] Grimm RA, Stewart WJ, Arheart K, Thomas JD, Klein AL. Left atrial appendage ‘stunning’ after electrical cardioversion of atrial flutter: an attenuated response compared with atrial fibrillation as the mechanism for lower susceptibility to thromboembolic events. *J Am Coll Cardiol* 1997;29:582–9.
- [52] Kam RM, Garan H, McGovern BA, Ruskin JN, Harthorne JW. Transient right bundle branch block causing R wave attenuation postdefibrillation. *Pacing Clin Electrophysiol* 1997;20:130–1.
- [53] Hasdemir C, Shah N, Rao AP, Acosta H, Matsudaira K, Neas BR, et al. Analysis of troponin I levels after spontaneous implantable cardioverter defibrillator shocks. *J Cardiovasc Electrophysiol* 2002;13:144–50.
- [54] Osswald S, Trouton TG, O’Nunain SS, Holden HB, Ruskin JN, Garan H. Relation between shock-related myocardial injury and defibrillation efficacy of monophasic and biphasic shocks in a canine model. *Circulation* 1994;90:2501–9.
- [55] Jones JL, Jones RE, Balasky G. Microlesion formation in myocardial cells by high-intensity electric field stimulation. *Am J Physiol* 1987;253:H480–6.
- [56] Peleska B. [Problems of defibrillation and stimulation of the myocardium]. *Zentralbl Chir* 1965;90:1174–88.
- [57] Nikolski VP, Sambelashvili AT, Krinsky VI, Efimov IR. Effects of electroporation on optically recorded transmembrane potential responses to high-intensity electrical shocks. *Am J Physiol Heart Circ Physiol* 2004;286:H412–8.
- [58] Gurvich NL. The main principles of cardiac defibrillation. Moscow Russia: Medicine; 1975.
- [59] Ohuchi K, Fukui Y, Sakuma I, Shibata N, Honjo H, Kodama I. A dynamic action potential model analysis of shock-induced aftereffects in ventricular muscle by reversible breakdown of cell membrane. *IEEE Trans Biomed Eng* 2002;49:18–30.